

***Final Draft***  
**of the original manuscript:**

Farhan, M.; Rudolph, T.; Kratz, K.; Lendlein, A.:  
**Torsional Fiber Actuators from Shape-memory Polymer.**  
In: MRS Advances. Vol. 3 (2018) 63, 3861 - 3868.  
First published online by Cambridge University Press: November 29, 2018

DOI: 10.1557/adv.2018.621  
<https://dx.doi.org/10.1557/adv.2018.621>

# Torsional Fiber Actuators from Shape-memory Polymer

Muhammad Farhan<sup>1,2</sup>, Tobias Rudolph<sup>1</sup>, Karl Kratz<sup>1</sup>, Andreas Lendlein<sup>1,2\*</sup>

<sup>1</sup>*Institute of Biomaterial Science and Berlin-Brandenburg Center for Regenerative Therapies, Helmholtz-Zentrum Geesthacht, 14513 Teltow, Germany;*

<sup>2</sup>*Institute of Chemistry, University of Potsdam, 14476 Potsdam, Germany*

\*corresponding author: [andreas.lendlein@hzg.de](mailto:andreas.lendlein@hzg.de)

## ABSTRACT:

Humanoid robots, prosthetic limbs and exoskeletons require soft actuators to perform their primary function, which is controlled movement. In this work, we explored whether crosslinked poly[ethylene-co-(vinyl acetate)] (cPEVA) fibers, with different vinyl acetate (VA) content can serve as torsional fiber actuators, exhibiting temperature controlled reversible rotational changes. Broad melting transitions ranging from 50 to 90 °C for cPEVA18-165 or from 40 to 80 °C for cPEVA28-165 fibers in combination with complete crystallization at temperatures around 10 °C make them suitable actuating materials with adjustable actuation temperature ranges between 10 and 70 °C during repetitive cooling and heating. The obtained fibers exhibited a circular cross section with diameters around 0.4±0.1 mm, while a length of 4 cm was employed for the investigation of reversible rotational actuation after programming by twist insertion using 30 complete rotations at a temperature above melting transition. Repetitive heating and cooling between 10 to 60 °C or 70 °C of one-end-tethered programmed fibers revealed reversible rotations and torsional force. During cooling 3±1 complete rotations ( $\Delta\theta = + 1080\pm360^\circ$ ) in twisting direction were observed, while 4±1 turns in the opposite direction ( $\Delta\theta = - 1440\pm360^\circ$ ) were found during heating. Such torsional fiber actuators, which are capable of approximately one rotation per cm fiber length, can serve as miniaturized rotary motors to provide rotational actuation in futuristic humanoid robots.

## INTRODUCTION:

Fiber actuators are materials or devices that can reversibly contract or rotate within one component as response to an external stimulus [1, 2]. The combination of rotation and contraction could also lead to various types of complex motions (e.g. bending, by contracting one side of the material while expanding the other side). Though currently in limited use, fiber actuators have the potential to be a highly disruptive emerging technology due to their high flexibility, versatility and high

power to weight ratio [3, 4]. The wide range of applications include humanoid robots, powered exoskeletons and active textiles [5-7]. Carbon nanotube (CNT) yarn has been reported as torsional and tensile actuators with fast, high-force, large-stroke tensile and torsional behaviors [8-10]. These CNT-based yarns could be realized as electrochemically operated torsional and rotational motors in the electrolyte as well as electrically, chemically and photonically powered hybrid yarn actuators [9]. CNT-based yarns are widely investigated, however scalability and higher costs have restricted their deployment. Shape-memory metal wires and polymer/CNT composite fibers could serve as artificial muscle fibers but they are hysteretic, expensive and must be redrawn/reprogrammed between cycles respectively [11-13].

Polymer yarns have also been recently introduced as stress-restricted artificial fiber muscles with high-stress and high-strength properties. It has been demonstrated that inexpensive high-strength polymer fibers used for fishing line and sewing thread (nylon) can be transformed by twist insertion to provide long-life tensile and torsional muscles utilizing the principle of thermal expansion and contraction [5, 14]. Such fiber materials have been shown as energy harvesters [15, 16] or in woven textiles that change porosity in response to temperature [5]. Recently, it was proposed that twisted fibers made from shape-memory polymers (SMPs) could potentially serve as tensile or torsional actuators similar to CNT-reinforced composite fibers [17]. Such polymeric actuators could provide another route to high-energy artificial muscles that respond to temperature changes.

Polymer networks with crystallizable segments have been reported capable of two-way shape-memory effects (2W-SMEs), when subjected to a constant stress during cyclic heating and cooling [18-20]. The working principle of such temperature-controlled polymer actuators is based on a melting induced contraction (MIC) and a crystallization induced elongation (CIE) during cyclic heating and cooling under a specific constant stress. Most recently, stimuli-responsive polymers capable of a free-standing reversible actuation have been reported [21-25]. Here polymer networks are required, which contain crystallizable actuation (AUs) as well as skeleton forming geometry determining units (GUs), and exhibit reversible actuation after orientation. In addition to their actuation capabilities, these polymer networks allow to introduce additional useful functions such as reprogrammability, self-healing, surface functionality and non-response temperature intervals [23, 26-28].

In this study, we hypothesized that reversible torsional actuation can be realized in crosslinked poly[ethylene-*co*-(vinyl acetate)] (cPEVA) fibers having a broad melting range. For such actuation,

fibers were programmed by twisting and reversible rotations of the one-end–tethered single fibers were investigated with reversible change in temperature. We speculated that by twist programming, the crystallites in such fibers can be oriented anisotropically along the twist direction, and in this way reversible rotations can be obtained by applying repetitive heating and cooling cycles. Some of these aligned crystals could be used to fix the twisted structure of the fibers; however others could be utilized to provide reversible rotational actuation. Thermo-mechanical properties of fibers were investigated by differential scanning calorimetry (DSC) and tensile tests at ambient as well as elevated temperatures; whereas the torsional actuation was analyzed from heat-cool cycles of free standing twisted single fibers.

## **MATERIALS AND METHODS:**

### **Materials**

Poly[ethylene-*co*-(vinyl acetate)] with a vinyl acetate content of 18 wt% (Elvax<sup>®</sup> 460A, DuPont, PEVA18) and of 28 wt% (Elvax<sup>®</sup> 260A, DuPont, PEVA28) were used in this study. Triallyl isocyanurate TAIC (99%) served as crosslinking agent from Sigma-Aldrich (Steinheim, Germany). Polymers and TAIC were used as received (without any purification).

### **Methods**

#### **Crosslinked Fiber Preparation**

Fibers were prepared from a mixture of 99 wt% of PEVA (PEVA18 or PEVA28) and 1 wt% of TAIC. At first, polymer granulates and crosslinking agent were mixed in a twin-screw extruder (Euro Prism Lab, Thermo Fisher Scientific, USA) at 110 °C and 50 rpm. In next step, the blend granulates (PEVA+TAIC) were extruded to obtain fibers with a diameter around 0.4±0.1 mm. Lastly, these fibers were crosslinked by gamma ( $\gamma$ ) beam irradiation at BGS (Beta-Gamma-Service GmbH & Co. KG, Wiehl, Germany) to achieve 165 kGy dosage. Sample ID were given based on different VA content of the starting thermoplastic polymer, such as 18 and 28 followed by a three digits representing the different irradiation dose, for example cPEVA18-165.

#### **Differential Scanning Calorimetry (DSC)**

DSC measurements were performed on a calorimeter (Netzsch, Selb, Germany) DSC 204, with heating and cooling rate of 10 K·min<sup>-1</sup>. Thermal data reported correspond to the second heating,

whereas the area under the melting and crystallization peaks led to calculate the corresponding enthalpies. Weight percentage (wt%) crystallinity was calculated as described in **Equation 1**.

$$\chi_c = \frac{\Delta H_m}{\Delta H_m^\circ/100} * 100\% \quad (1)$$

where  $\Delta H_m^\circ/100$  is enthalpy of melting of 100% crystalline polymer, which is 287 J·g<sup>-1</sup> for polyethylene [29].

### **Cyclic thermomechanical torsional tests**

For reversible torsional actuation evaluation, cPEVA28 fibers were programmed by twisting at 80 °C and cPEVA18 at 90 °C (in a Zwick Z1.0 with a thermo-chamber and temperature controller) followed by cooling below crystallization temperatures. The crosshead speed was 3 rpm and selected sample length was 4 cm. Fibers were programmed to ( $\theta_{prog} \approx 10800^\circ$ ) equivalent to 30 turns (one turn/twist = 360° rotation) per total length (4 cm). After programming, the samples were hanged freely in a closed glass cylinder with a temperature sensor (to avoid direct air flow on the fiber). Heating and cooling cycles were performed inside the thermo-chamber in order to have a proper temperature control. Three cycles were conducted to investigate the actuation performance. The reversible rotations of the fibers were recorded by a camera and analysed. The reversible rotation angle during cooling (+) and heating (-) were calculated [ $\Delta\theta_r = \theta_{T,low} - \theta_{T,high}$ ]. Three heating and cooling cycles were recorded for each sample, different  $T_{high}$  60 or 70 °C were used for cPEVA28 and cPEVA18 fibers respectively, while similar  $T_{low} = 10$  °C was selected. The reversible rotations of the fibers were recorded (videos) and analysed. For further torsional characteristics, the relative reversible change in rotational angle ( $\theta'_{rev}$ ) and twist fixation efficiency ( $W_{ef}$ ) can be calculated as

$$\theta'_{rev} = \frac{\theta_{T,low} - \theta_{T,high}}{\theta_{T,high}} * 100\% \quad (2)$$

$$W_{ef} = \frac{\theta_{T,high}}{\theta_{T,prog}} * 100\% \quad (3)$$

Where  $\theta_{T,high}$  and  $\theta_{T,low}$  are the angles at  $T_{high}$  and  $T_{low}$  respectively, while  $\theta_{prog}$  is programming angle. Descriptive statistics were applied for the analysis of obtained data, where the presented results are average values from the repeated experiments. The standard deviation in reversible rotational actuation is based on the different cycles within one experiment.

## RESULTS AND DISCUSSION:

A broad melting transition from 50 to 90 °C was observed for cPEVA18-165 with melting peaks maxima around  $T_m = 81 \pm 2$  °C. Similarly, cooling thermograms show a broad crystallization with peak maxima around  $T_c = 61 \pm 2$  °C. The cPEVA28-165 fibers exhibit lower  $T_m = 66 \pm 2$  °C as well as  $T_c = 43 \pm 2$  °C with the melting transition ranging from 40 to 80 °C. The crystallinity ( $\chi_c$ ) calculated from melting enthalpy was also higher  $\chi_c = 26 \pm 2\%$  for cPEVA18-165 when compared to cPEVA28-165, which exhibit lower  $\chi_c = 17 \pm 1\%$ . Reversible torsional actuation was achieved in twisted fibers as shown in figure 1. For this purpose, a suitable set of parameters for programming and reversible actuation cycles were selected from thermo-mechanical investigation. The programming step included twisting of fibers in a completely amorphous state, e.g., at 90 °C for cPEVA18, while at 80 °C for cPEVA18 followed by cooling to 0°C. A cyclic temperature  $T_{high} = 70$  °C was selected for cPEVA18-165. Here, the crystallites with  $T_m < 70$  °C can act as actuation domains to provide reversible rotational actuation, while crystallites with  $T_m > 70$  °C act as geometry determining domains for the stabilization of twisted structure of fibers during actuation. Lower  $T_{high} = 60$  °C was selected for the set of cPEVA28 fibers as a result of lower melting range. The cyclic temperature  $T_{low} = 10$  °C was selected below the crystallization temperature.

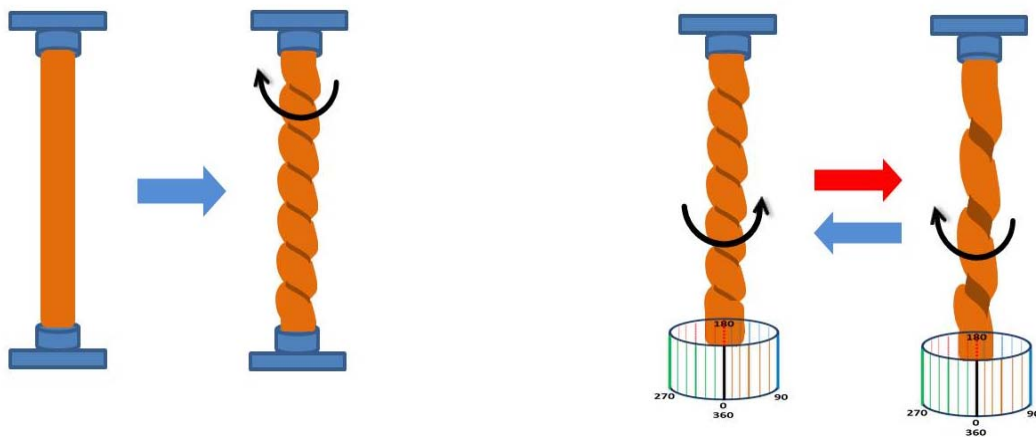


**Figure 1:** Schematic illustration of the free-standing torsional actuation of single fiber, programming by twisting is shown on left, the reversible rotation of the freely hanged (one-end-tethered) fiber is demonstrated on right.

The number of twists for programming were selected from the breaking strength of the samples on twisting (similar as elongation at break for cyclic tensile measurements), which was investigated above  $T_m$  and characterized by the number of twists required to break a fiber. For this purpose, fiber samples with 4 cm length were held in the Zwick machine with thermo-chamber, where one

end of the fiber was fixed, while the other end could be rotated in clockwise direction. cPEVA28-165 as well as cPEVA18-165 fibers were investigated by twisting until break at 80 or 90 °C, respectively. Both fiber samples broke around  $35 \pm 2$  turns, therefore 30 turns were selected for programming. To observe free-standing reversible rotations, the programmed fiber samples were freely hanged and reversibly heated and cooled to the defined  $T_{\text{high}}$  and  $T_{\text{low}}$ . Three reversible cycles were employed for such investigations. The picture series for the free-standing torsional effect of such fibers is presented in figure 2 for three consecutive cycles, where the movement could be realized by the rotation of the metal hook attached to the free-standing fiber.

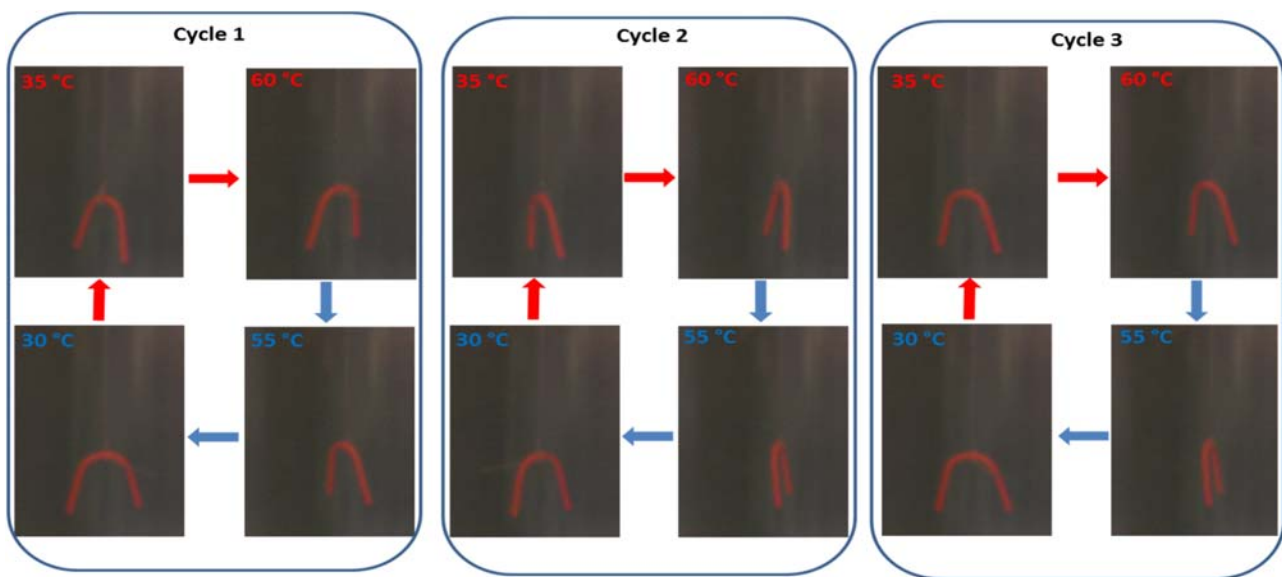


**Figure 2:** Picture series of three heating and cooling cycles of cPEVA28-165, to visualize the movement a red colored hook is attached to freely hanging polymer fiber, 1) un-twisting on heating in clock wise direction, 2) re-twisting on cooling in anti-clock wise direction.

Heating led to the melting of the crystals and rotation in one direction, while cooling involves the crystallization in the twist direction, consequently rotation in the opposite direction. The changes in the twist fiber can be realized in figure 3c. The number of rotations observed in different fibers was in the range of 3 to 4 complete turns in the heating step in 4 cm twisted fiber, resulting in approximately one rotation per cm. However, rotation during cooling was slow and some samples showed a slight reduced number of rotations in the cooling step, which might be attributed to the increased stiffness of the fiber on cooling. Since the diameter of the fibers was in the similar range and all the fibers were programmed with similar number of twists, the effect of fiber diameter and number of twists in programming on the actuation performance was not observed. The changes in

angle in heating and cooling were recorded by taking snapshots from movies and the data is shown as two separate plots in figure 3a and figure 3b for cPEVA18-165 and cPEVA28-165 respectively.

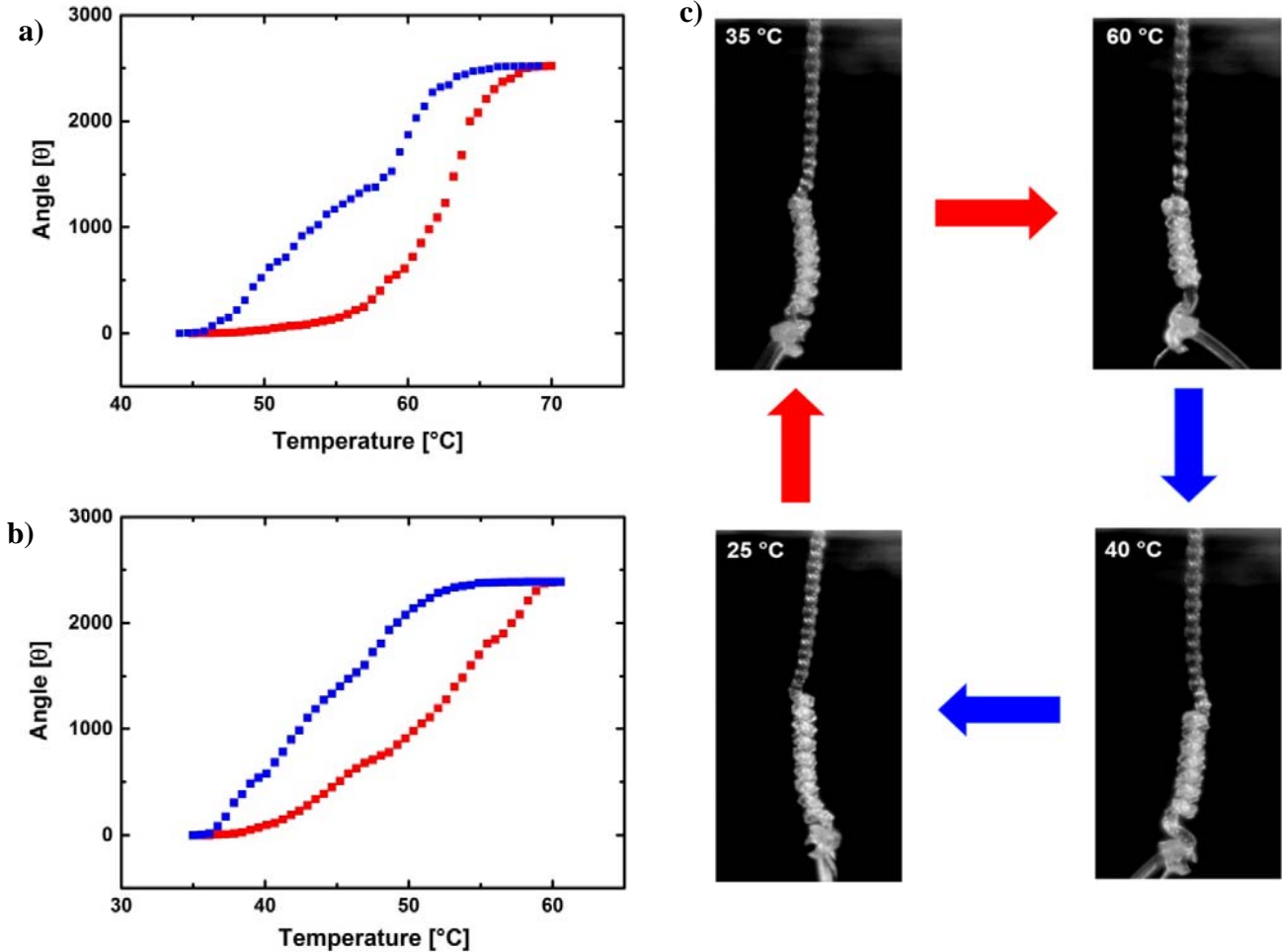


**Figure 3:** Reversible change in angle in 2<sup>nd</sup> cycle during heating (red) and cooling (blue) of **a)** cPEVA18-165kGy and **b)** cPEVA28-165kGy, the data are taken from picture series generated from movie. **c)** Picture series showing changes in the fiber during cyclic heating and cooling.

The observed reversible rotational angle ( $\Delta\theta$ ) in cooling and heating was  $\Delta\theta = + 1440\pm 360^\circ$  and  $\Delta\theta = - 1080\pm 360^\circ$  respectively for cPEVA18-165. Relatively fast actuation/rotation was noticed from 58 to 68 °C in cPEVA18-165, while irreversible rotations were realized when heated  $\geq 75$  °C. A comparable reversible torsional actuation performance was observed for cPEVA28-165. Furthermore, relative reversible change in rotational angle ( $\theta'_{rev}$ ) and twist fixation efficiency ( $W_{ef}$ ) were calculated by analysing the videos as described in experimental section. The observed data



revealed a higher  $\theta'_{\text{rev}} = 42 \pm 1$  and lower  $W_{\text{ef}} = 51 \pm 2$  for cPEVA28-165 when compared to cPEVA18-165, where a slightly reduced  $\theta'_{\text{rev}} = 34 \pm 1$  and higher  $W_{\text{ef}} = 56 \pm 2$  were obtained.

## CONCLUSIONS:

Crosslinked cPEVA fibers could be programmed as free-standing torsional actuators, showing their ability to reversibly rotate with change in external temperature, which can serve as an alternate to expensive carbon nanotube yarn actuators. One-end-tethered twisted fibers were reversibly heated and cooled in a close cylinder to investigate reversible rotation. The twisted fibers demonstrated almost equal reversible rotations for several heating and cooling cycles with approximately  $4 \pm 1$  rotations during heating and  $3 \pm 1$  rotations during cooling step in 4 cm fiber length. By selection of the suitable  $T_{\text{high}}$  within the PE melting transition interval, the twist geometry of the fibers could be sustained during heating and cooling cycles, by sufficient amount of PE crystals having higher  $T_{\text{m}}$ . The rotating geometry of these fibers can be erased by heating above melting transition and can be reprogrammed by stretching to give tensile actuation. This approach could be extended to the variety of the polymers to achieve different transition temperature for specific applications. Such temperature controlled rotating or contracting fiber actuators can provide low cost artificial fiber muscles for humanoid robotics and for reversibly shape changing textiles.

## Acknowledgement:

This work was supported by the Helmholtz-Association through programme-oriented funding. The authors thank Mr. Robert Bendisch and Dr. Hans-Jürgen Kosmella for technical support. M. Farhan acknowledges the German Federal Ministry for Education and Research (BMBF, Grant No.031A095) for financial support.

## REFERENCES

1. S. M. Mirvakili, A. Pazukha, W. Sikkema, C. W. Sinclair, G. M. Spinks, R. H. Baughman and J. D. W. Madden, *Adv Funct Mater* **23** (35), 4311-4316 (2013).
2. G. V. Stoychev and L. Ionov, *Acs Appl Mater Inter* **8** (37), 24281-24294 (2016).
3. F. Carpi, R. Kornbluh, P. Sommer-Larsen and G. Alici, *Bioinspir Biomim* **6** (4), 1748-3182 (2011).
4. Y. Bar-Cohen, *Proc Spie* **9056** (2014).
5. C. S. Haines, M. D. Lima, N. Li, G. M. Spinks, J. Foroughi, J. D. W. Madden, S. H. Kim, S. L. Fang, M. J. de Andrade, F. Goktepe, O. Goktepe, S. M. Mirvakili, S. Naficy, X. Lepro, J. Y. Oh, M. E. Kozlov, S. J. Kim, X. R. Xu, B. J. Swedlove, G. G. Wallace and R. H. Baughman, *Science* **343** (6173), 868-872 (2014).

6. B. Tondou, S. Ippolito, J. Guiochet and A. Daidie, *Int J Robot Res* **24** (4), 257-274 (2005).
7. Q. W. Shi, J. H. Li, C. Y. Hou, Y. L. Shao, Q. H. Zhang, Y. G. Li and H. Z. Wang, *Chem Commun* **53** (81), 11118-11121 (2017).
8. C. H. Kwon, K. Y. Chun, S. H. Kim, J. H. Lee, J. H. Kim, M. D. Lima, R. H. Baughman and S. J. Kim, *Nanoscale* **7** (6), 2489-2496 (2015).
9. M. D. Lima, N. Li, M. J. de Andrade, S. L. Fang, J. Oh, G. M. Spinks, M. E. Kozlov, C. S. Haines, D. Suh, J. Foroughi, S. J. Kim, Y. S. Chen, T. Ware, M. K. Shin, L. D. Machado, A. F. Fonseca, J. D. W. Madden, W. E. Voit, D. S. Galvao and R. H. Baughman, *Science* **338** (6109), 928-932 (2012).
10. J. Foroughi, G. M. Spinks, G. G. Wallace, J. Oh, M. E. Kozlov, S. L. Fang, T. Mirfakhrai, J. D. W. Madden, M. K. Shin, S. J. Kim and R. H. Baughman, *Science* **334** (6055), 494-497 (2011).
11. H. Koerner, G. Price, N. A. Pearce, M. Alexander and R. A. Vaia, *Nat Mater* **3** (2), 115-120 (2004).
12. P. Miaudet, A. Derre, M. Maugey, C. Zakri, P. M. Piccione, R. Inoubli and P. Poulin, *Science* **318** (5854), 1294-1296 (2007).
13. S. M. Mirvakili and I. W. Hunter, *Acs Appl Mater Inter* **9** (19), 16321-16326 (2017).
14. S. Aziz, J. Foroughi, H. R. Brown and G. M. Spinks, *J Polym Sci Pol Phys* **54** (13), 1278-1286 (2016).
15. S. H. Kim, M. D. Lima, M. E. Kozlov, C. S. Haines, G. M. Spinks, S. Aziz, C. Choi, H. J. Sim, X. M. Wang, H. B. Lu, D. Qian, J. D. W. Madden, R. H. Baughman and S. J. Kim, *Energ Environ Sci* **8** (11), 3336-3344 (2015).
16. S. H. Kim, H. J. Sim, J. S. Hyeon, D. Suh, G. M. Spinks, R. H. Baughman and S. J. Kim, *Sci Rep-Uk* **8** (2018).
17. J. K. Yuan and P. Poulin, *Science* **343** (6173), 845-846 (2014).
18. T. Chung, A. Rorno-Urbe and P. T. Mather, *Macromolecules* **41** (1), 184-192 (2008).
19. J. Zotzmann, M. Behl, D. Hofmann and A. Lendlein, *Advanced Materials* **22** (31), 3424-3429 (2010).
20. Q. X. Yang, J. Z. Fan and G. Q. Li, *Appl Phys Lett* **109** (18) (2016).
21. T. Gong, K. Zhao, W. X. Wang, H. M. Chen, L. Wang and S. B. Zhou, *J Mater Chem B* **2** (39), 6855-6866 (2014).
22. Y. Meng, J. S. Jiang and M. Anthamatten, *Acs Macro Lett* **4** (1), 115-118 (2015).
23. A. Lendlein, *Science Robotics* **3** (18) (2018).
24. M. Behl, K. Kratz, U. Nochel, T. Sauter and A. Lendlein, *P Natl Acad Sci USA* **110** (31), 12555-12559 (2013).
25. M. Behl, K. Kratz, J. Zotzmann, U. Nöchel and A. Lendlein, *Advanced Materials* **25** (32), 4466-4469 (2013).
26. M. Farhan, S. R. Chaganti, U. Nochel, K. Kratz and A. Lendlein, *Polym Advan Technol* **26** (12), 1421-1427 (2015).
27. M. Farhan, T. Rudolph, U. Nochel, W. Yan, K. Kratz and A. Lendlein, *Acs Appl Mater Inter* **9** (39), 33559-33564 (2017).
28. M. Farhan, T. Rudolph, U. Nochel, K. Kratz and A. Lendlein, *Polymers-Basel* **10** (3) (2018).
29. F. M. Mirabella and A. Bafna, *J Polym Sci Pol Phys* **40** (15), 1637-1643 (2002).